Fluorescent Probes

DOI: 10.1002/anie.201305784

Development of Azo-Based Fluorescent Probes to Detect Different Levels of Hypoxia**

*Wen Piao, Satoru Tsuda, Yuji Tanaka, Satoshi Maeda, Fengyi Liu, Shodai Takahashi, Yu Kushida, Toru Komatsu, Tasuku Ueno, Takuya Terai, Toru Nakazawa, Masanobu Uchiyama, Keiji Morokuma, Tetsuo Nagano, and Kenjiro Hanaoka**

Hypoxia is due to an inadequate supply of oxygen in the body, and is associated with various diseases.[1] In some solid tumors, for example, the median oxygen concentration has been reported to be around 4%, and locally, it may even decrease to 0%.[2] This induces various biological phenomena, such as the stabilization of the hypoxia-inducible factor 1α (HIF-1α) and the modulation of HIF-mediated gene expression.[3,4] Therefore, methods to detect and visualize hypoxia are important for investigating its biological effects. Several organic molecular probes have been used as indicators of hypoxia. For example, pimonidazole contains a nitroaryl group that is selectively reduced by reductases under hypoxia.[5] However, detection requires immunostaining of the reduction product, and this method is thus not applicable to living cells.

On the other hand, reaction-based fluorescent probes can be powerful tools to elucidate processes in living systems,[6] and several hypoxia-sensing fluorescent probes have been developed to detect hypoxia in living cells.[7] Most of them contain a nitroaryl or a quinone group as the hypoxia-sensitive moiety. The photoswitching mechanism of these probes is mostly based on a photoinduced electron transfer (PeT) mechanism, but it is susceptible to environmental conditions, such as pH or polarity.[8,9] Furthermore, some of these probes employ fluorophores that are known to be pH-sensitive. Therefore, a new design strategy is required to develop more reliable and versatile tools.

Recently, we reported that an azo group has excellent properties as a hypoxia-sensitive moiety, and we developed a hypoxia-sensitive fluorescent probe QCy5[10] that makes use of the reduction of an azo group under hypoxia.[11] However, this fluorescent probe still entailed some drawbacks. First, QCy5 responds only to very low oxygen concentrations (less than 1% O_2; Supporting Information, Figure S1). However, hypoxic responses do not always occur only under such severe conditions, so higher sensitivity is desirable. Second, QCy5 utilizes the Förster resonance energy transfer (FRET) mechanism for the off/on switching of fluorescence, and the fluorescence quencher, Black Hole Quencher 3 (BHQ-3), which contains an azo group, is used as the hypoxia-sensitive moiety. This quencher, however, is not susceptible to further chemical modification. Indeed, to the best of our knowledge, there has been only one report of a chemical modification of BHQ-3, and even in that case, the basic scaffold was not changed.[12] As we wished to develop a series of probes with different colors that would be suitable for the detection of different levels of hypoxia, a different probe design was needed that would not require the use of BHQ-3. For this purpose, we focused on the photophysical properties of azo compounds. In general, azo dyes, such as azobenzene derivatives, are nonfluorescent owing to ultrafast conformational change around the N=N bond after photoexcitation.[13] Although this photophysical property of azo compounds is well-known, to the best of our knowledge, there has been no attempt to conjugate an azo moiety directly to the conjugated system of a fluorophore to quench the fluorescence. We thought that this simple idea would be useful for the development of a variety of hypoxia-sensitive probes, because reductive cleavage of the azo bond would restore fluorescence by regenerating the original fluorophore (Figure 1). Such a strategy should significantly extend the scope of hypoxia sensors with controllable off/on switching of the

[*] W. Piao, S. Takahashi, Y. Kushida, Dr. T. Komatsu, Dr. T. Ueno, Dr. T. Terai, Prof. M. Uchiyama, Prof. T. Nagano, Dr. K. Hanaoka
Graduate School of Pharmaceutical Sciences
The University of Tokyo
7-3-1 Hongo, Bunkyo-ku, Tokyo 113-0033 (Japan)
E-mail: khanaoka@mol.f.u-tokyo.ac.jp
S. Tsuda, Dr. Y. Tanaka, Prof. T. Nakazawa
Department of Ophthalmology, Tohoku University
Graduate School of Medicine
1-1 Seiryo-machi, Aoba-ku, Sendai, Miyagi 980-8574 (Japan)
Dr. S. Maeda
Department of Chemistry, Faculty of Science, Hokkaido University
Kita 10 Nishi 8, Kita-ku, Sapporo, Hokkaido 060-0808 (Japan)
Dr. F. Liu, Prof. K. Morokuma
Fukui Institute for Fundamental Chemistry, Kyoto University
34-4 Takano Nishihiraki-cho, Sakyo, Kyoto 606-8103 (Japan)
Prof. M. Uchiyama
Advanced Elements Chemistry Laboratory
RIKEN 2-1 Hirosawa, Wako-shi, Saitama 351-0198 (Japan)

[**] This work was supported in part by MEXT (Specially Promoted Research Grant 22000006 to T.N., 24689003 and 24659042 to K.H., and 24655147 to T.K.) and SENTAN and JST(K.H.). K.H. was also supported by The Asahi Glass Foundation, The Uehara Memorial Foundation, the Tokyo Biochemical Research Foundation, the Inoue Foundation for Science, the Takeda Science Foundation, and The Cosmetology Research Foundation. The authors thank Mr. Yu Harabuchi of Hokkaido University for helpful discussions on photoreactions of azobenzene. Some of the theoretical calculations were carried out using the computational resources of the Institute for Molecular Science, Okazaki (Japan). W.P. was supported by a Grant-in-Aid for JSPS Fellows.

Supporting information for this article is available on the WWW under http://dx.doi.org/10.1002/anie.201305784.

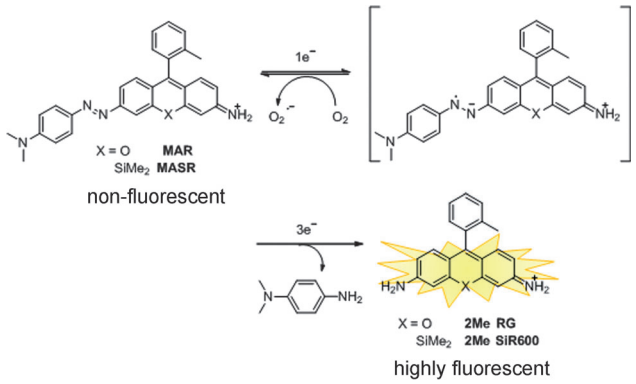

Figure 1. Design strategy, chemical structure, and proposed detection mechanism for azo rhodamines (MAR and MASR).

fluorescence to afford probes that respond to different levels of hypoxia. Herein, we report the development of novel fluorescent probes that employ this new, non-FRET-based photo switching concept, with a scaffold amenable to chemical modification.

Rhodamine derivatives were employed as scaffold fluorophores, because there are numerous reports of fluorescent probes that are based on this fluorophore, and chemical modification is straightforward.[14] 2Me rhodamine green (2Me RG) and 2Me Si-rhodamine 600 (2Me SiR 600)[15] were employed as scaffold fluorophores for fluorescent probes (Figures 1, S2 and Table 1). 2Me RG is a derivative of rhodamine green that is obtained by converting the carboxylic acid substituent into a methyl group to increase its hydrophobicity, thus affording higher cell-membrane permeability. 2Me SiR 600 is a red fluorescent dye that we recently developed, in which the oxygen atom in the xanthene moiety of 2Me RG is replaced by a dimethylsilyl group. Both of these dyes are insensitive to a change in pH in the range of pH 3.0–10.0, and exhibit high fluorescence emission (Figure S3). Based on these fluorophores, we designed mono-azo rhodamine (MAR) and mono-azo Si-rhodamine (MASR; Figure 1).

Table 1: Photophysical Properties in PBS at pH 7.4

Dye	λ_{abs} [nm]	λ_{fl} [nm]	ε [$M^{-1}cm^{-1}$]	Φ_{fl}[a]
2Me RG	498	520	8.2×10^4	0.84
2Me SiR 600	593	613	9.1×10^4	0.38
MAR	601	n.d.	3.8×10^4	<0.001
MASR	427	n.d.	2.0×10^4	<0.001

[a] For the determination of the fluorescence quantum efficiency (Φ_{fl}), fluorescein in NaOH solution (0.1 N; $\Phi_{fl}=0.85$) was used for 2Me RG and MAR, and rhodamine B in EtOH ($\Phi_{fl}=0.65$) was used for 2Me SiR 600 and MASR as fluorescence standards. n.d. = not detectable, PBS = phosphate-buffered saline.

We conducted quantum-chemical calculations to examine whether quenching would occur through an ultrafast conformational change of the N=N bond of these fluorescent probes (Figure S4), as seen for azo systems such as azobenzene.[13d] To simplify the calculations, we employed a model molecule of MAR, namely a MAR derivative without the methylbenzene moiety. We first confirmed that the molecular orbitals and vertical excitation energies for the model molecule were very similar to those obtained for MAR (Figure S4a). Moreover, for the model molecule, the oscillator strengths to the S_1 and S_2 states are 0.0030 and 1.7647, respectively; these values are in good agreement with those for MAR (0.0085 and 1.7015, respectively; Table S1). In both systems, excitations to S_1 and S_2 correspond mainly to $n\rightarrow\pi^*$ (HOMO−2→LUMO and LUMO+1) and $\pi\rightarrow\pi^*$ (HOMO→LUMO) transitions, respectively (Table S1). The results of the calculations also indicate that excitation almost exclusively occurs to the S_2 state, judging from the oscillator strength (Table S1). Starting from the S_2 state, the system moves to the S_1 state through the S_2/S_1 conical intersection (CI), then it undergoes C–N=N–C bond rotation at the S_1 state, and the system finally reaches the S_0 state through a S_1/S_0 CI (Figure S4b,c). In the case of azobenzene, a complicated $S_2\rightarrow S_1$ pathway that involves higher excited states was proposed, as S_2 ($\pi\rightarrow\pi^*$) and S_1 ($n\rightarrow\pi^*$) do not cross near the initial (S_0-MIN) geometry.[16] However, in the present case, the S_2/S_1 CI is very close to the initial geometry, and the decay simply occurs through it. There is a very small barrier on S_1 (1.9 kJ mol^{-1} from S_1-MIN to S_1-TS), which is negligible compared to the excitation energy to S_2. Overall, the potential-energy profile is generally downhill along the present pathway (for potential energy curves along the path, see Figures S5 and S6). Thus, once excited to the S_2 state, the system is expected to decay very quickly to the S_0 state without emission. Based on the high similarity between MAR and the model molecule, we consider it very likely that a similar ultrafast radiationless decay also occurs in MAR.

To synthesize the fluorescent probes, we converted one amino group of the xanthene moiety of the fluorophores into an azo group by means of an azo coupling reaction.[17] This reaction provided the desired fluorescent probes, MAR and MASR. As expected, these two compounds showed no fluorescence (Table 1; see also Table S2 and Figure S7), were unaffected by a change in pH between pH 3.0 and 10.0 (Figure S8), and possess high photostability (Figure S9). The absorption spectrum of MASR in a phosphate buffer at pH 7.4 indicated a less intense absorbance at approximately 620 nm, when compared to the spectrum recorded in $CHCl_3$ (Figure S10). This might be the result of nucleophilic attack of the hydroxide ion at the 9 position of the xanthene moiety.[15] These results indicate that our design strategy is a promising method to control the off/on switching of fluorescence for hypoxia sensors.

To examine whether these probes can detect hypoxia in biological systems, we first conducted an in vitro assay using rat liver microsomes, which contain various reductases. After adding NADPH (50 μM) as a cofactor for the reductases to aqueous solutions of MAR or MASR (1 μM) in the presence of rat liver microsomes (226 μg/3 mL), a rapid increase in the fluorescence intensity of MAR or MASR was observed only under hypoxia with an initial reaction rate of 1.1×10^{-3} μM s^{-1} or 2.1×10^{-3} μM s^{-1}; the fluorescence intensity increased by 630-fold or 20-fold, respectively (Figure 2). The absorption

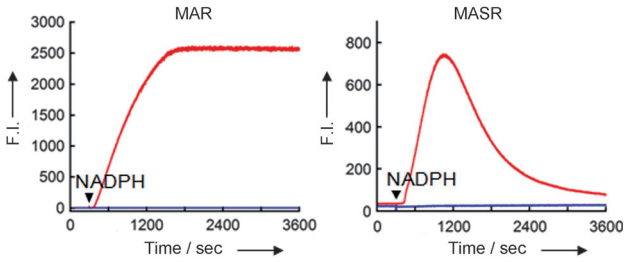

Figure 2. Time-dependent changes in the fluorescence intensity of MAR or MASR (1 μM) in the presence of rat liver microsomes (226 μg/3 mL) under hypoxia (——) or normoxia (——). Measurements were performed in a potassium phosphate buffer (0.1 M; pH 7.4) containing DMSO (0.1%) as a cosolvent. As a cofactor for reductases, NADPH (50 μM) was added after 5 min. The hypoxic conditions were prepared by bubbling argon gas into the reaction solution for 30 min. The excitation and emission wavelengths were 498 and 520 nm for MAR, and 593 and 612 nm for MASR, respectively.

spectra also indicated that the reduction proceeded only under hypoxia (Figure S11). We further confirmed that the fluorophores, 2Me RG or 2Me SiR 600, were generated from MAR or MASR under hypoxia by HPLC analysis of the reaction mixtures (Figure 1; see also Figure S12). Furthermore, these probes showed a negligible fluorescence increase in the presence of an excess of GSH, hydrogen sulfide, or reactive oxygen species (ROS), which are generated during reperfusion (Figure S13).[18] In the case of MASR, a fluorescence intensity decrease occurred after approximately 1000 seconds (Figure 2), and we considered this observation to be due to the reduction of the fluorophore itself (2Me SiR 600), as a similar fluorescence intensity decrease was observed when 2Me SiR 600 was incubated with microsomes under hypoxia (Figure S14). This can explain the weak absorbance increment at approximately 610 nm that is seen after reduction under hypoxic conditions (Figure S11b). As replacing the oxygen atom with a dimethylsilyl moiety lowers the LUMO energy level of the xanthene moiety,[19,20] 2Me SiR 600 is more susceptible to reduction than 2Me RG. Nevertheless, no significant decrease in fluorescence intensity was observed when cells were incubated with 2Me SiR 600 under hypoxia (Figure S15). This result indicates that MASR, as well as 2Me SiR 600, is practical and useful for live-cell fluorescence imaging.

We next applied these probes to living cells to monitor cellular hypoxia. Under hypoxia (0.1% O_2), a time-dependent increase in fluorescence intensity was observed in A 549 cells, whereas almost no fluorescence enhancement inside cells was seen under normoxia (Figure S16). For both probes, their low toxicity was confirmed by a live/dead staining assay (Figure S17). The flavoprotein inhibitor diphenyliodonium chloride (DPI)[21] dramatically suppressed the fluorescence increase both in the cuvette and in cells (Figure S18). Despite the low specificity of the inhibitor, this result suggests that these probes are reduced by flavoproteins, such as NADPH-cytochrome P450 reductase, which are thought to be responsible for the metabolic activation of bioreductive compounds under hypoxia.[22] Intriguingly, we found that MAR and MASR showed different sensitivities to oxygen concentration: As evaluated by fluorescence microscopy imaging, the fluorescence intensity of MASR increased at oxygen concentrations of 1% or less, whereas that of MAR increased at oxygen concentrations of 5% or less, which corresponds to relatively mild hypoxia (Figure 3). Pimonidazole is reported to detect hypoxia at oxygen concentrations of 10 mmHg (1.3%) or less;[23] thus, whereas MASR, like QCy 5, is suitable

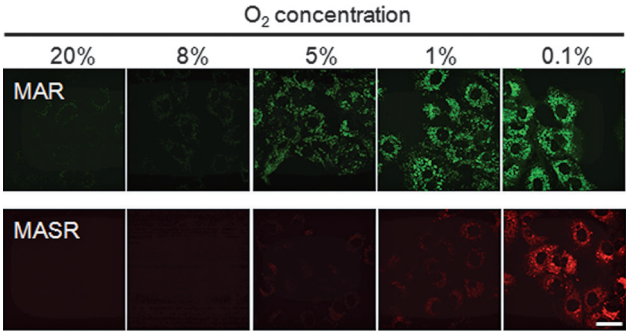

Figure 3. Fluorescence confocal microscopy images of MAR or MASR in live A 549 cells. A 549 cells were incubated with MAR or MASR (1 μM) containing DMSO (0.1%) as a cosolvent at various oxygen concentrations for six hours. Scale bar: 30 μm. The excitation and emission wavelengths were 488 and 515–553 nm for MAR, and 600 and 620–700 nm for MASR, respectively.

for the detection of severe hypoxia, MAR features a higher sensitivity and can detect mild hypoxia, as compared to pimonidazole (Figure S19). This oxygen concentration dependency of the fluorescence intensity increase of MAR and MASR was also confirmed by flow-cytometric analysis (Figure S20). The same oxygen concentration dependency of MAR and MASR was observed in both HeLa cells and Colon 26 cells (Figure S21), as well as in A 549 cells. Although the chemical structures of MAR and MASR are similar, the localizations of the scaffold fluorophores, 2Me RG and 2Me SiR 600, inside cells were different: 2Me RG was localized in the mitochondria, whereas 2Me SiR 600 was mainly localized inside the lysosomes (Figure S22). Thus, we speculate that the localizations of MAR and MASR inside cells are also different, and that this may at least partially influence their sensitivity to the oxygen concentration.

Based on the above findings, we next tried to visualize the oxygen gradient in cultured cells under a cover glass using both MAR and MASR, as it has been reported that mounting a thin quartz cover glass on top of cultured cells can create an oxygen gradient.[24] The cover glass prohibits oxygen supply from above, so that the oxygen concentration gradually decreases with the distance from the edge of the cover glass (Figure 4a). A 549 cells were simultaneously loaded with both MAR and MASR, then a cover glass was placed on top. We observed that the fluorescence intensities of MAR (green channel) and MASR (red channel) gradually increased with increasing distance from the edge of the cover glass (Figure 4b), whereas almost no fluorescence enhancement was observed in the absence of the cover glass (Figure S23). Strong fluorescence of both MAR and MASR was observed from cells at the center of the cover glass, while only

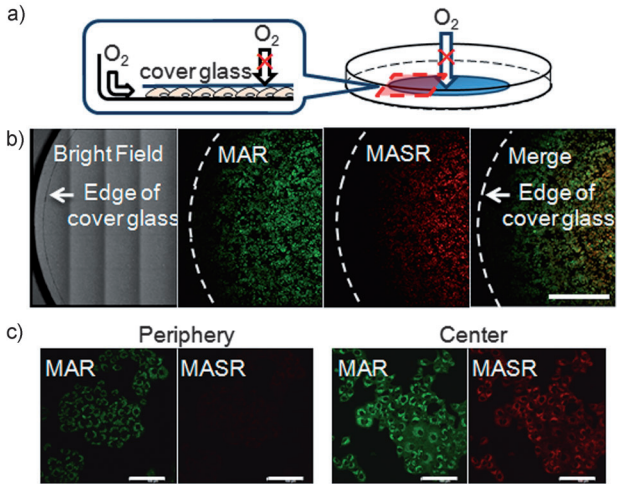

Figure 4. Detection of a gradient of cellular hypoxia generated by placing a cover glass on top of the cells. a) Cellular hypoxia being caused by the cover glass. b) Bright-field and fluorescence confocal microscopy images of A549 cells onto which the cover glass was placed. Cells were incubated under normal culture conditions with the cover glass for three hours in the presence of MAR (0.5 μM) and MASR (1 μM) containing DMSO (0.15%). Twenty images were combined into one image with the Leica SP5 software. Scale bar: 2.5 mm. c) Magnified images of A549 cells near the boundary of the cover glass (periphery) and in the central part of the cover glass (center). Scale bar: 100 μm. The excitation and emission wavelengths were 488 and 515–553 nm for MAR, and 600 and 620–700 nm for MASR, respectively.

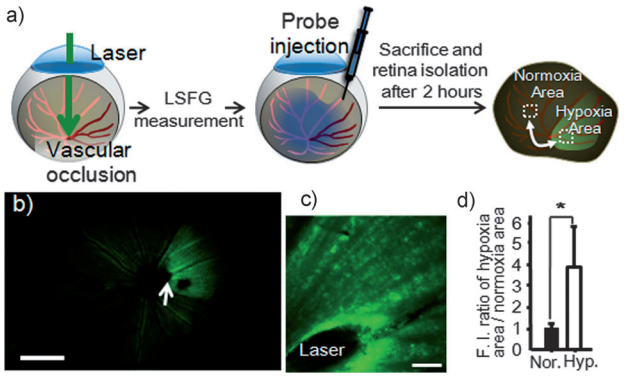

Figure 5. Fluorescence imaging of branch retinal artery occlusion (BRAO) in a rat model with MAR. a) Hypoxia imaging method after BRAO. MAR (2 mM, 2 μL) was injected into the vitreous humor of a BRAO model rat, and the retinal whole-mount was observed under a fluorescence microscope. b, c) Fluorescence imaging of the isolated retina two hours after MAR treatment with a low (b)- or high (c)-magnification lens. Scale bars: 1 mm (b) and 100 μm (c). The arrow in (b) indicates the point of laser irradiation. d) Comparison of the fluorescence intensities observed in hypoxic and normoxic areas ($n = 6$, * Mann–Whitney U test, $p = 0.007$).

fluorescence of MAR was detected for cells closer to the edge of the cover glass (Figure 4c). Although it is still difficult to quantify the oxygen concentration, the combined use of the two probes allows the visualization of the oxygen-concentration gradient by means of multicolor imaging.

Finally, we attempted to visualize retinal hypoxia in a rat model of retinal artery occlusion, where rapid development of retinal ischemia quickly damages the inner layer neurons.[25] We used MAR in this experiment, because it is more sensitive to hypoxia than MASR. The rat model of branch retinal artery occlusion (BRAO) was prepared by intravenous administration of the photosensitizing dye Rose Bengal, followed by green-laser irradiation of a retinal artery (Figure 5a).[25b,26] BRAO was confirmed by observing the blood flow in the retinal vessels before and after BRAO with laser speckle flowgraphy (LSFG), which can noninvasively measure the blood-flow velocity in the choroid, retina, and optic nerve head (Figure S24).[27] After BRAO, MAR was injected into the vitreous humor, and two hours later, the rat was sacrificed for histological observation. The fluorescence intensity in the area of retinal hypoxia was higher than that in a normoxic area (Figure 5b). The cells of the inner retinal layer in the area were stained (Figure 5c). In this fluorescence image, the mean ratio of the fluorescence brightness in the area of retinal hypoxia was $389.8 \pm 189.8\%$ (mean ± SD), which was significantly higher than that in the area of retinal normoxia ($100.0 \pm 17.2\%$; Figure 5d). These results indicate that MAR can be a useful tool to detect hypoxia not only in vitro, but also in vivo.

In conclusion, by taking advantage of the photochemical properties of an azo bond, which include sensitivity to hypoxia, we have developed two novel fluorescent probes, MAR and MASR, which are based on a new photo switch concept to detect hypoxia. Owing to quenching by ultrafast azo-bond rotation after photoexcitation, MAR and MASR showed no fluorescence, which was supported by quantum-chemical calculations. Reduction of MAR or MASR by reductases under hypoxia resulted in the generation of highly fluorescent rhodamine derivatives, 2Me RG or 2Me SiR600, respectively, accompanied by a large enhancement in the fluorescence intensity. Thus, direct conjugation of an azo group to the conjugated system of the fluorophore is a useful design strategy for hypoxia-sensitive fluorescent probes. Furthermore, MAR and MASR showed different hypoxia detection thresholds: Their fluorescence intensity increased as the oxygen concentration fell below 5% and 1%, respectively. Multicolor imaging with both probes allowed us to visualize the oxygen concentration gradient in living cells under a cover glass. Moreover, we showed that MAR could visualize retinal hypoxia in a rat model of retinal artery occlusion. Thus, we believe MAR and MASR will be practically useful tools for investigating a variety of hypoxia-related biological phenomena. Because of their simple chemical structures, further chemical modification would be straightforward. Our strategy should also be applicable to the development of a range of hypoxia-sensitive probes with different threshold levels.

Received: July 4, 2013
Published online: October 14, 2013

Keywords: azo compounds · bioorganic chemistry · fluorescent probes · imaging agents · oxygen concentration

[1] G. L. Semenza, *N. Engl. J. Med.* **2011**, *365*, 537 – 547.
[2] P. Vaupel, K. Schlenger, C. Knoop, M. Höckel, *Cancer Res.* **1991**, *51*, 3316 – 3322.
[3] U. Lendahl, K. L. Lee, H. Yang, L. Poellinger, *Nat. Rev. Genet.* **2009**, *10*, 821 – 832.
[4] N. Rohwer, T. Cramer, *Drug Resist. Updates* **2011**, *14*, 191 – 201.
[5] J. A. Raleigh, C. J. Koch, *Biochem. Pharmacol.* **1990**, *40*, 2457 – 2464.
[6] J. Chan, S. C. Dodani, C. J. Chang, *Nat. Chem.* **2012**, *4*, 973 – 984.
[7] a) Y. Liu, Y. Xu, X. Qian, J. Liu, L. Shen, J. Li, Y. Zhang, *Bioorg. Med. Chem.* **2006**, *14*, 2935 – 2941; b) L. Cui, Y. Zhong, W. Zhu, Y. Xu, Q. Du, X. Wang, X. Qian, Y. Xiao, *Org. Lett.* **2011**, *13*, 928 – 931; c) K. Xu, F. Wang, X. Pan, R. Liu, J. Ma, F. Kong, B. Tang, *Chem. Commun.* **2013**, *49*, 2554 – 2556; d) H. Komatsu, H. Harada, K. Tanabe, M. Hiraoka, S. Nishimoto, *MedChemComm* **2010**, *1*, 50 – 53; e) S. Zhang, M. Hosaka, T. Yoshihara, K. Negishi, Y. Iida, S. Tobita, T. Takeuchi, *Cancer Res.* **2010**, *70*, 4490 – 4498; f) E. Nakata, Y. Yukimachi, H. Kariyazono, S. Im, C. Abe, Y. Uto, H. Maezawa, T. Hashimoto, Y. Okamoto, H. Hori, *Bioorg. Med. Chem.* **2009**, *17*, 6952 – 6958; g) Z. Li, X. Li, X. Gao, Y. Zhang, W. Shi, H. Ma, *Anal. Chem.* **2013**, *85*, 3926 – 3932.
[8] Y. Urano, D. Asanuma, Y. Hama, Y. Koyama, T. Barrett, M. Kamiya, T. Nagano, T. Watanabe, A. Hasegawa, P. L. Choyke, *Nat. Med.* **2008**, *15*, 104 – 109.
[9] H. Sunahara, Y. Urano, H. Kojima, T. Nagano, *J. Am. Chem. Soc.* **2007**, *129*, 5597 – 5604.
[10] K. Kiyose, K. Hanaoka, D. Oushiki, T. Nakamura, M. Kajimura, M. Suematsu, H. Nishimatsu, T. Yamane, T. Terai, Y. Hirata, T. Nagano, *J. Am. Chem. Soc.* **2010**, *132*, 15846 – 15848.
[11] S. Zbaida, *Drug Metab. Rev.* **1995**, *27*, 497 – 516.
[12] A. Chevalier, C. Massif, P. Renard, A. Romieu, *Chem. Eur. J.* **2013**, *19*, 1686 – 1699.
[13] a) I. K. Lednev, T.-Q. Ye, P. Matousek, M. Towrie, P. Foggi, F. V. R. Neuwahl, S. Umapathy, R. E. Hester, J. N. Moore, *Chem. Phys. Lett.* **1998**, *290*, 68 – 74; b) M. Poprawa-Smoluch, J. Baggerman, H. Zhang, H. P. A. Maas, L. De Cola, A. M. Brouwer, *J. Phys. Chem. A* **2006**, *110*, 11926 – 11937; c) J. Yoshino, N. Kano, T. Kawashima, *Chem. Commun.* **2007**, 559 – 561; d) H. M. D. Bandara, S. C. Burdette, *Chem. Soc. Rev.* **2012**, *41*, 1809 – 1825.
[14] a) Y.-H. Ahn, J.-S. Lee, Y.-T. Chang, *J. Am. Chem. Soc.* **2007**, *129*, 4510 – 4511; b) L. D. Lavis, T.-Y. Chao, R. T. Raines, *ACS Chem. Biol.* **2006**, *1*, 252 – 260; c) J. Li, S. Q. Yao, *Org. Lett.* **2009**, *11*, 405 – 408; d) M. Sakabe, D. Asanuma, M. Kamiya, R. J. Iwatate, K. Hanaoka, T. Terai, T. Nagano, Y. Urano, *J. Am. Chem. Soc.* **2013**, *135*, 409 – 414; e) S. Kenmoku, Y. Urano, H. Kojima, T. Nagano, *J. Am. Chem. Soc.* **2007**, *129*, 7313 – 7318.
[15] Y. Kushida, K. Hanaoka, T. Komatsu, T. Terai, T. Ueno, K. Yoshida, M. Uchiyama, T. Nagano, *Bioorg. Med. Chem. Lett.* **2012**, *22*, 3908 – 3911.
[16] I. Conti, M. Garavelli, G. Orlandi, *J. Am. Chem. Soc.* **2008**, *130*, 5216 – 5230.
[17] E. Merino, *Chem. Soc. Rev.* **2011**, *40*, 3835 – 3853.
[18] a) G. L. Baker, R. J. Corry, A. P. Autor, *Ann. Surg.* **1985**, *202*, 628 – 641; b) B. C. Dickinson, C. J. Chang, *Nat. Chem. Biol.* **2011**, *7*, 504 – 511.
[19] S. Yamaguchi, K. Tamao, *J. Chem. Soc. Dalton Trans.* **1998**, 3693 – 3702.
[20] Y. Koide, Y. Urano, K. Hanaoka, T. Terai, T. Nagano, *ACS Chem. Biol.* **2011**, *6*, 600 – 608.
[21] a) S. Chakraborty, V. Massey, *J. Biol. Chem.* **2002**, *277*, 41507 – 41516; b) V. B. O'Donnell, G. C. Smith, O. T. Jones, *Mol. Pharmacol.* **1994**, *46*, 778 – 785; c) D. G. Tew, *Biochemistry* **1993**, *32*, 10209 – 10215.
[22] W. R. Wilson, M. P. Hay, *Nat. Rev. Cancer* **2011**, *11*, 393 – 410.
[23] J. A. Raleigh, S. C. Chou, G. E. Arteel, M. R. Horsman, *Radiat. Res.* **1999**, *151*, 580 – 589.
[24] E. Takahashi, M. Sato, *Am. J. Physiol. Cell Physiol.* **2010**, *299*, C1318 – 1323.
[25] a) S. Kuroiwa, N. Katai, H. Shibuki, T. Kurokawa, J. Umihira, T. Nikaido, K. Kametani, N. Yoshimura, *Invest. Ophthalmol. Visual Sci.* **1998**, *39*, 610 – 617; b) L. Daugeliene, M. Niwa, A. Hara, H. Matsuno, T. Yamamoto, Y. Kitazawa, T. Uematsu, *Invest. Ophthalmol. Visual Sci.* **2000**, *41*, 2743 – 2747.
[26] a) F. Moroni, G. Lombardi, S. Pellegrini-Faussone, F. Moroni, *Vision Res.* **1993**, *33*, 1887 – 1891; b) Y. Zhang, C.-H. Cho, L. Atchaneeyasakul, T. McFarland, B. Appukuttan, J. T. Stout, *Invest. Ophthalmol. Visual Sci.* **2005**, *46*, 2133 – 2139.
[27] Y. Tamaki, M. Araie, E. Kawamoto, S. Eguchi, H. Fujii, *Exp. Eye Res.* **1995**, *60*, 373 – 383.

